

Assessing Intel’s Memory Bandwidth Allocation for resource limitation in real-time systems

Giorgio Farina¹, Gautam Gala², Marcello Cinque¹, Gerhard Fohler²

(1) Università degli Studi di Napoli Federico II, Italy

(2) Technische Universität Kaiserslautern, Germany

{giorgio.farina,macinque}@unina.it {gala,fohler}@eit.uni-kl.de

Abstract—Industries are recently considering the adoption of cloud computing for hosting safety critical applications. However, the use of multicore processors usually adopted in the cloud introduces temporal anomalies due to contention for shared resources, such as the memory subsystem. In this paper we explore the potential of Intel’s Memory Bandwidth Allocation (MBA) technology, available on Xeon Scalable processors. By adopting a systematic measurement approach on real hardware, we assess the indirect memory bandwidth limitation achievable by applying MBA delays, showing that only given delay values (namely 70, 80 and 90) are effective in our setting. We also test the derived bandwidth assured to a hypothetical critical core when interfering cores (e.g., generating a concurrent memory access workload) are present on the same machine. Our results can support designers by providing understanding of impact of the shared memory to enable predictable progress of safety critical applications in cloud environments.

Index Terms—Real-time, Temporal contention, Memory Bandwidth Allocation, Access limitation

I. INTRODUCTION

As seen in Ericson’s Computing Fabric [8], and railway use case of EU projects such as SECREDAS [9], industries are exploring cloud computing and virtualization for hosting safety-critical applications [7] as clouds support ease of re-usability, maintainability, and reconfiguration while providing workload elasticity and higher availability. Thus, clouds help industries in reducing their running costs and carbon footprint. Industries can execute existing safety-critical applications without any significant modifications as Virtual Machines (VMs) in a cloud computing environment. These safety-critical VMs must run alongside other non-critical/best-effort VMs executing in the cloud. All VMs are unaware that they are running in a virtualized environment or know the actual underlying cloud nodes or hardware resources, thanks to the virtualization (abstraction) provided by the hypervisor.

Cloud nodes are based on COTS multicore processors, which are rich in shared resources to allow fast communication and improve the average resource utilization. Nevertheless, sharing introduces new forms of non-determinism and dependencies (in space and time) between parallel flows complicating the analysis of the Worst-Case Execution Time (WCET), which is fundamental for safety-critical applications.

Recent research on real-time hypervisors focused mainly on CPU virtualization, adopting either hierarchical scheduling [23] or CPU partitioning [22], and implementing cache

coloring [16] to reduce inter-core cache interference in multi-cores. However, open problems regarding temporal contention (and consequent unexpected delays) are still observed when tasks/VMs co-executing on different cores need to access the memory (controller) simultaneously.

Memory access contention deserves special attention for two main reasons: (i) memory accesses are unavoidable, and, contrarily to other sources of temporal contention [15] [21], (ii) memory access interference can increase the WCET by several orders of magnitude, particularly when increasing the number of co-accessing cores [18], [20]. The picture is even more complex on modern multicore architectures for cloud computing where many cores (or hardware threads) share additional resources such as a Last Level Cache (LLC). For instance, the spatial contention in the LLC has a significant impact on the memory access contention as LLC writebacks lead to asynchronous memory accesses. While memory accesses are synchronous with respect to the requester demand, asynchronous memory accesses (e.g., due to LLC writebacks) may depend on the memory requests from other cores, as the LLC is shared.

Existing work proposes several memory access regulation methods to limit the maximum interference for the worst case memory access latency analysis. The basic idea is to limit the memory accesses from individual cores for each regulation period [25] [17]. Thus, it is possible to distribute the available memory access bandwidth and obtain a tighter worst case memory access latency bound. Software-based resource limitation approaches, such as Memguard [25], require monitoring the memory requests (or cache misses) from each core and applying a throttling policy to prevent memory accesses from cores that have depleted the assigned memory budget for that regulation period. Despite the design simplicity of software-based approaches, it is not possible to achieve high resolution and efficiency due to the coarse-grained regulation period duration and high overheads. In addition, the throttling policy of the approaches involve stalling the core execution to prevent memory accesses. Such a throttling policy is not suitable for cloud VMs as a core cannot continue its execution within the private context, such as private caches and functional units, reducing the private resources utilization.

A possible way to overcome the limitations of software-based approaches is to rely on hardware support. In this respect, Intel recently proposed a new hardware feature known

as Memory bandwidth allocation (MBA) present in Xeon Scalable processors [10], depicted in Fig. 1. MBA delays the requests going to the interconnect from a core’s private context. Intel provides nine values between 10 to 90 in increments of 10 representative of the delays that are inserted between the requests. MBA can be used to apply indirect memory bandwidth throttling overcoming the limitations of software base-approaches as: (1) we have a fine-grained regulation period because the delays are inserted by hardware between requests (2) a hardware based method does not require software intervention, except for the initial setup, to partition memory bandwidth statically (3) the core execution is not stalled to prevent memory access, thus preserving the private resource utilization.

Despite these promising features, it is still unclear if and how MBA can be used for memory regulation to provide real-time guarantees to safety-critical VMs. As a matter of fact, the MBA controller does not directly allocate memory bandwidth to cores, and hence the memory bandwidth allocation/regulation is an indirect consequence of the introduced delay.

In this paper, we present the results of a measurement study performed on Intel Xeon Scalable processors in order to derive the indirect memory bandwidth achieved by the cores through MBA for providing real-time guarantees. The main contributions and results of the study are:

- 1) We propose a systematic approach to derive the indirect memory bandwidth limitation from delay values using a single-core analysis where we highlight the importance to consider also L2 writebacks within the design of experiments;
- 2) We experimentally prove that only the 70, 80 and 90 MBA delay values are effective in our setting at limiting the memory bandwidth even in the presence of LLC write-backs (asynchronous memory accesses);
- 3) We test the derived assured memory fetching latency for a core allocated to a critical VM when MBA limits the bandwidth of three interfering cores with a multicore analysis, showing the potential and effectiveness of the approach.

The rest of the paper is structured as follows. Section II presents the related work, while the background on new Intel MBA feature is provided in Section III. Our design of experiments is presented in Section IV, while Sections V and VI presents the results of single-core and multicore analysis, respectively. Finally Section VII ends the paper with final remarks and hints for future work.

II. RELATED WORK

The management of memory access time interference can be broadly classified in two approaches (extending the classification in [13]): (i) interference estimation, to take it into account in worst case execution time analysis, and (ii) interference regulation by either enforcing execution models or limiting the access to the memory controller at runtime. In the following we review the literature falling into these two categories.

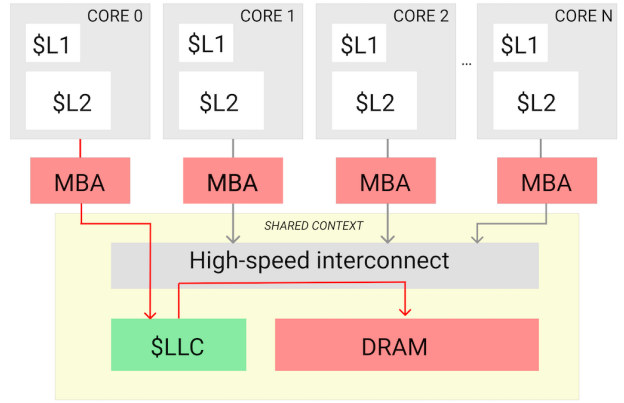


Fig. 1. Abstract model of Intel Xeon memory hierarchy depicting the MBA controller between the cores and high-speed interconnect

A. Interference Estimation Approaches

The idea is to analytically estimate the maximum number of conflicts through static analysis. Under a worst-case perspective, the first goal is to classify accesses depending on the addressed hierarchical memory level. Such analysis gets complicated with shared caches. In [14] each access is first analyzed in the absence of inter-core cache conflicts, and subsequently, a separate inter-core cache conflict analysis refines each classified access. [5] improves the estimation of inter-core cache conflicts combining abstract interpretation and path-sensitive verification (e.g., model checking and symbolic execution). In [6], [12], [4] shared cache and bus analysis are combined, applying a time-division bus arbitration. Estimation approaches suffer from several drawbacks. First, the computational complexity increases with the number of tasks. Second, the arbiter is supposed to be deterministic, enabling time-division multiple access (TDMA). However, this is not possible on modern COTS due to their optimization policies. Third, there are no independent partitions: the estimation validity is strictly coupled with the tasks under analysis.

B. Interference Regulation Approaches

1) *Approaches based on execution models:* The basic idea of execution models is to split real-time tasks into different phases and then enforce a high-level co-scheduling mechanism. The co-scheduler rules implicitly define the contention degree without relying on low-level arbiters. The memory accesses are then serialized in several phases, and these phases can be overlapped by the co-scheduler achieving a predictable degree of interference. In [19], [3] the co-scheduler implements a TDMA policy. In particular, the work in [19] proposes PREM handling the contention of main memory between a single-core and several peripherals. Whereas, the work in [3] extends the concept of the execution model to a multicore platform dividing the execution phase into communication and local execution slices.

Execution models are invasive, as they require program or

compiler modifications. Moreover, the TDMA policy is not scalable with the number of cores.

2) *Approaches based on resource limitation*: The aim of these approaches is to make the maximum interference predictable and deterministic, by limiting the processing element accesses, with no modification to the original program. These solutions are usually based on a throttling policy to stop the processing element access in case of excessive request, and a monitoring policy for counting the issued requests.

Notably, [2] are among the first ones to perceive the potentiality of performance counters to monitor shared resource accesses. The idea is to capture on each processing element (PE) the only interesting available events, such as last-level cache hits and references to extract the number of LLC misses (representing synchronous accesses). Nowadays, LLC misses are supported as non-architectural events on modern COTS and are also used to monitor PE accesses, [24], [25].

As throttling policy, [1] inserts idle-loops inside TLB-miss handler, while the works in [24], [25] propose to deschedule the task. The work in [18] starts from the computation of the *interference-sensitive* WCET taking into account a safety bound for shared-resource interference when at runtime resource capacity enforcement is used to limit the actual resource usage of each process, which are executed following a round robin scheduling scheme. Such pessimistic model is based on a strong assumption on the interference delays.

As software-based resource limitation approaches present the already mentioned efficiency and resolution issues, in the rest of the paper we focus on the new capabilities offered by Intel's MBA technology.

III. NEW INTEL CAPABILITIES

In this work we focus on the Intel Cascade-Lake micro-architecture, which inherited from the Skylake-Server micro-architecture an exclusive LLC and a mesh as a network of interconnect. An LLC exclusive frees the last level cache to be as large as the sum of all core private caches, saving the private cache size scalability (i.e., we went from 254KB to our 1MB L2 cache size). At the same time, the mesh allows higher parallelism in the memory access and last level cache. It is important to take into account the exclusivity property of the LLC when designing the workload for the measurements (see next section). An exclusive LLC does not include all private cache lines, improving the overall cache space utilization. Such property influences the handling in response to an LLC miss where the new fetched cache line is not brought in LLC to keep the inclusivity.

The considered micro-architecture, as well as all the new Intel Xeon processors, supports temporal and spatial isolation at the hardware level through Resource Director Technology (RDT) [11]. We can associate spatial and temporal properties with a class of service (CLOS) and then bind the CLOS to a virtual core.

One physical core cannot change the class of service of another core. However, it can configure the properties of any CLOS. RDT makes available monitoring and allocation features.

RDT allocation features enable inter-core resource partitioning. While the Cache Allocation Technology (CAT) and Code and Data Prioritization (CDP) deal with the LLC spatial partitioning, the Memory Bandwidth Allocation (MBA) addresses the temporal memory contention. The MBA controls a configurable delay for requests going to the network of interconnect from the core private context. By configuring such delays, we can apply an indirect limitation in memory access without impacting the use of private resources such as private caches and functional units. Operationally, a MBA delay value can be associate with a class of service (CLOS), e.g., to limit the memory bandwidth of cores hosting non-critical VMs. If two virtual cores of the same physical core have different delays, the larger delay will override the other. In our case, disabling the Hyper Threading (HP) in the experiments, we have a side effect [10]; in particular, the non-active hardware threads are assigned to the CLOS0 by default even though they are disabled. Hence, the CLOS0 has not been used. Otherwise, the hidden delay value of the non-active virtual core (the delay value associated with the CLOS0) overrides the MBA delay value of the active virtual machine on the same physical core when the first is higher than the second one.

IV. DESIGN OF EXPERIMENTS

We design a set of experiments to perform two main analyses. The single-core analysis is based on a systematic approach to deriving the indirect memory bandwidth limitation achieved when the MBA delays the requests. Contrarily, the multi-core analysis is focused on the guarantees rather than the limitation. Multi-core analysis tests the memory bandwidth achieved by a core executing a critical VM when the MBA (indirectly) limits memory accesses from 3 interfering cores (performing best-effort tasks). Both, single-core and multi-core analysis, share the following architectural parameters (Table I). We use only one socket (one processor) composed of eight cores at most. We set the number of active cores via BIOS configuration. We only used one memory channel in both analyses. We set the DRAM refresh rate to periodic and the CPU core frequency to maximum (no power saving) in the BIOS. These parameters helped keep the latency variability to a minimum and maximize the memory requests rate. Similarly, we disabled the Pre-fetcher and Hyperthreading to reduce variability since hardware threads on the same physical core share the same "queue" to the memory, while the prefetcher can preload several lines after a single cache miss. Experiments are conducted on an Intel Xeon Silver processor, Cascade-Lake microarchitecture, with 8 cores, 2,10 GHz, 512KB L1 cache (256KB out of 512 KB are dedicated for the Code), 1MB L2 cache, and 11MB LLC. Next subsections present the design of experiments for both analyses. Our measures achieve the 99% of accuracy calculated as the 99% mean confidence interval using a student's t distribution divided by the sample mean.

TABLE I
DESIGN OF EXPERIMENTS: SHARED PARAMETERS

Shared parameters	setting
Sockets no.	1
Used DRAM channel	1
Prefetcher	disabled
SMT	disabled
DRAM refresh cycles	periodic
Core frequency	Maximum

TABLE II
DESIGN OF EXPERIMENTS: SINGLE-CORE ANALYSIS

Parameters	setting
Cores no.	1
Factors	values
MBA delay	$d \in D, D = \{10; 40; 50; 60; 70; 80; 90\}$
Workload	$k \in K, K = \{R^I; R^{II}; W^{II}\}$
	$R^I: \{$ 8192 CAS R, no L2WBs, no LLCWBs }
	$R^{II}: \{$ 8192 CAS R, with L2WBs, no LLCWBs }
	$W^{II}: \{$ 8192 CAS R, with L2WBs, with LLCWBs }
Metric	description
Memory fetching latency	memory fetching latency in terms of CPU cycles $L_{k;d}, k \in K, d \in D$

A. Single-core analysis

Single-core analysis has the objective to estimate the memory access limit for an interfering core when MBA is enabled with different delays. We exclude 20 and 30 delays from the analysis as they are erroneous on our processor (as reported in an Intel errata [10]) and produce the same results as delay value 10. Table II describes the design of experiments of the single-core analysis. Our experiments measure the latency execution variability for different kinds of workloads: memory read workload considers only synchronous memory accesses, while memory write workload accounts also the asynchronous memory writes. One of the main contributions is to specialize the memory read workload regarding the L2 writebacks as motivated later. The number of observations achieves more than 99% of accuracy.

1) *Memory read workload*: A read request in the worst case corresponds to a memory read operation when there is an LLC miss. Since we consider this worst-case in our workload, read request and memory read operation are interchangeable terms. However, we identify two different L2 traffic patterns for this worst-case due to the LLC exclusivity in the processor.

In the exclusive architecture, L2 writebacks (L2WBs) to the LLC happen whenever new memory is read and the L2 set is full, even though the evicted L2 cache line is clean (contrarily to the inclusive architecture).

We include the two L2 traffic patterns as a factor motivating this choice in Fig.2 and Fig.3 where we fetch 2 MB of dynamic memory in several blocks of 64 KB when the MBA is disabled (0-delay) and enabled with 90-delay. While the above plot represents the latency (CPU cycles) for each block, the graph below shows the respective L2WBs for each fetched block.

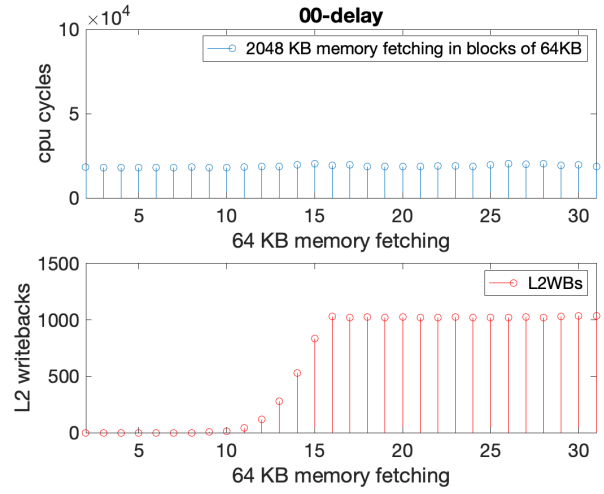


Fig. 2. 2048 KB memory fetching in several blocks of 64KB when the MBA is disabled (0-delay)

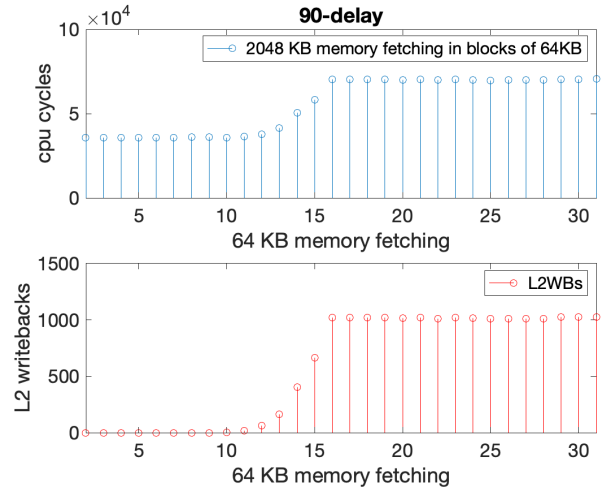


Fig. 3. 2048 KB memory fetching in several blocks of 64KB when the MBA 90-delay is enabled

The number of L2WBs grows as the L2 cache fills its capacity (L2 size is 1 MB). While initially, no L2WBs are observed (when L2 capacity is available), subsequently, when the L2 becomes full, each memory read will sure correspond to one L2WB (so 1024 memory reads of 64 bytes (64KB) generate 1024 L2 writebacks).

Looking at the figures, we have two main observations. (i) Without throttling (0-delay), the memory load latency does not change significantly when the L2WBs are present (Fig.2)¹. However, (ii) the latency changes when the MBA is enabled (Fig.3) on the two traffic patterns. From the results on CPU cycles, it is evident that the MBA delays the L2WBs requests, doubling the latency of read operations when writebacks are present. This might be possible because the controller

¹Note that our memory read workloads are designed to not cause LLC writebacks (LLCWBs)

should introduce a delay towards all outgoing requests on the interconnection network, thus also including reads and writes to the last level cache.

The second observation motivates us to consider L2 traffic pattern as a factor. The R^I and R^{II} in Table II represent the read workload respectively in the first (without L2WBs) and the second operational condition (with L2WBs). In particular, the read workload is composed of 8192 read requests where each request is an LLC miss ($readReqs = LLCmisses = CASReads = 8192$) and hence a memory read operation (CAS R is the command issued on the DRAM channel). The number of 8192 requests (meaning 512KB of memory fetching because each request retrieves 64 bytes which is the cache line size) has been chosen since it assures us to not have L2WBs in R^I ($L2WBs = 0$), given the L2 cache size of 1MB. This is also visible from Fig.2, where after 8 fetchings of 64 KB each, the number of L2WBs is still 0. On the opposite, in R^{II} the total L2 write-backs must be equal to the total memory requests ($L2WBs = 8192$). This is achieved by performing a pre-read workload to fill the L2 cache. Note that, considering the results in Fig.2 and Fig.3, R^I is the worst case workload (it has less limitation), since the frequency (latency) of memory reads is not reduced (delayed) by concurrent L2WBs.

As a side note, looking at Fig.3, we can observe that the MBA keeps the same limitation for each of the 1024 memory reads. Such workload in software-based approaches would require to set an infeasible regulation period of 10 microseconds, hence proving the better granularity offered by MBA-based approaches.

2) *Memory write workload*: We have memory writes in a writeback policy when a dirty LLC cache line is evicted. Hence, since our write workload reproduces the worst case, every request of the workload causes one memory read and one memory write operation, due to the cache line eviction and substitution. The W^{II} in Table II represents this kind of workload. In particular, the W^{II} workload is composed of 8192 requests where each request is the cause of one memory read, and one memory write ($writeReqs = LLCmisses = CASReads = CASWrites = 8192$). Only the second operational condition (II) is possible for the write workload since an LLC writeback can only be the result of a L2 writeback.

B. Multi-core analysis

While the single-core analysis gives us information about the memory access limitation when the MBA delay and workload are fixed, the multi-core analysis analyzes the assured memory fetching latency for a critical core when the MBA limits the accesses of the other cores. For our evaluation, we deploy a quad-core system where one of them is critical. In particular, we consider a specific case where the critical core fetches its dynamic memory without MBA limitation, reproducing a workload R^I . In contrast, the MBA limits the other three cores that perform the most permissive workload k' under limitation resulting by the single-core analysis. The range of delays considered for the interference cores range

TABLE III
DESIGN OF EXPERIMENTS: MULTI CORE ANALYSIS

Parameters	setting
crit. cores no.	1
crit. workload	R^I
int. cores no.	3
int. workload	the most permissive workload $k' \in K$ under D'
Factors	values
MBA delay	d_i for the i-th interference core $d_i \in D', i \in \{1; 2; 3\}$
Metric	description
Memory fetching latency	critical memory fetching latency in terms of CPU cycles $L_{k':(d_1, d_2, d_3)}$

from 10 to 90, however we will consider only significant ones D' , depending on the result of single-core analysis. The Table III describes the design of experiments. The multi-core analysis requires thirty observations to achieve a 99% of accuracy.

C. Measurement tool and workload considerations

We performed experiments in Linux as the high server boot duration (several minutes) makes it time-consuming to do bare-metal development and experimentation.

Our measurement tool captures the latency and several factors (such as LLC writeback, L2 writeback, and CAS commands) of a particular workload. The latency is captured in terms of TSC (Timestamp counter). The fixed TSC frequency is close to the maximum CPU frequency. Hence, we refer to TSC cycles as CPU cycles. We favor the latency rather than bandwidth measurements because the latter requires a regulation period limiting the resolution.

We maximize the interference writing the workload as consecutive memory operations (full-loop unrolling) and choosing a stride between consecutive accesses equal to the cache line size (our cache line size is 64 Bytes). Even though the loop unrolling of memory requests increases the code size, we design our experiments controlling the absence of extra LLC misses.

We reproduce the L2 traffic patterns for a read workload through initial setup operations. To avoid L2 writebacks and to have memory accesses, we flush the dynamic memory before the workload execution, while to reproduce L2 writebacks for the R^{II} workload, we also perform a pre-read workload to fill the L2 cache, as previously mentioned.

Contrarily, for the write workload W^{II} , we reproduce the worst-case executing a pre-workload of write-requests filling the entire cache space of dirty and useless cache-lines. In addition to synchronous memory accesses, the previous injected dirty cache lines assure LLC writeback (memory write) whenever an LLC eviction occurs.

V. RESULTS FROM THE ONE-CORE ANALYSIS

This section describes the single-core analysis results where the main goal was to estimate the indirect limitation of

memory bandwidth when the MBA is enabled. Below, we represent our results for the three workloads R^I , R^{II} , W^{II} .

A. Results representation

$L_{k;d}$ is the execution latency of the workload k when the d MBA delay is active.

Fig. 4 shows the $L_{k;d}$ boxplots for each experiment of Table II and a mean interpolation for the observations of the same workload and different MBA delays.

Observing the boxplot width, the latency variability is the same (or lower) when the limitation is enabled or not (0-delay). Hence, the MBA seems to be not a new source of variability. The main source of that variability is the periodic DRAM refresh cycles.

B. Results interpretation

The Fig. 4 shows two effects clearly. The first is that the limitations have not an important impact on the relative 0-delay observations until the 70-delay in our setting. The second is that the boxplots of workload R^{II} and W^{II} overlap for high delays, meaning a similar behavior due to L2WBs.

To better interpret the results from Fig. 4 for the 70, 80, and 90 delays, we prefer to go from the latency to bandwidth domain. Being T the minimum execution latency $\min(L_{R^I;0})$ to synchronously fetch 8192 cache lines (our chosen reference, as explained earlier), we calculate the achievable bandwidth (memory operations in T) of a generic configuration $k;d$, where k is the workload, and d is the delay, as:

$$BW_{k;d} = \frac{T * 8192}{L_{k;d}};$$

We report in Table IV the maximum observed bandwidth for delays from 60 to 90.

We evaluate also the maximum percentage of synchronous bandwidth as

$$\max(BW_{k;d})\% = \frac{\max(BW_{k;d}) * 100}{8192}$$

Note that the synchronous memory bandwidth could be lower than the achievable memory bandwidth as also memory writes are accounted (i.e., the workload W^{II} achieves 155% of synchronous bandwidth with the less restrictive 60-delay limitation). This is due to the fact that, in the worst case set by our write workload, each write request causes one memory read and one memory write operation, due to the eviction. The "2x" in Table IV accounts for this double access regarding memory writes.

Observing the results in the table, we can note that:

$$\max(BW_{R^I;d}) > \max(BW_{R^{II};d}) \quad (1)$$

hence, the less restrictive limitation for a memory read workload is when there are no L2 writebacks, confirming what anticipated in the previous section. We can also note that:

$$\max(BW_{R^I;70:90}) \approx \max(BW_{W^{II};70:90}) \quad (2)$$

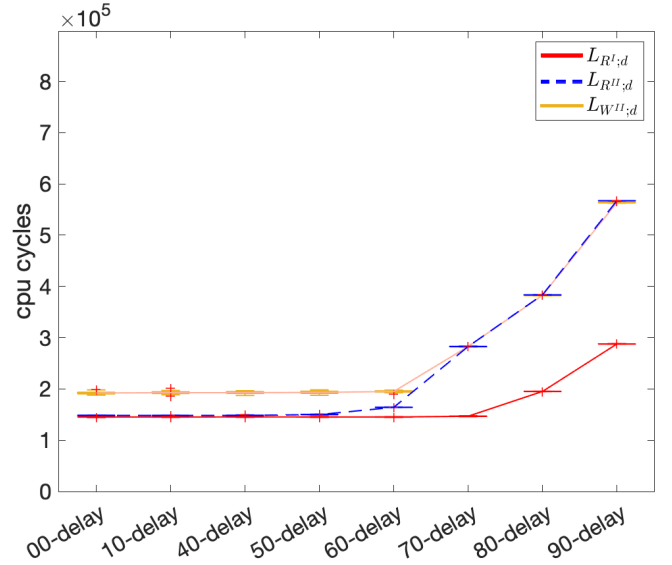


Fig. 4. Boxplot latencies for the different workloads and interpolation of the respective mean latencies

TABLE IV
THE MAXIMUM RATE AND THE PERCENTAGE OF SYNCHRONOUS MEMORY BANDWIDTH CORRESPONDING TO MINIMUM LATENCY (MEMORY OPERATIONS IN T).

Metrics	60-delay	70-delay	80-delay	90-delay
$\max(BW_{R^I;d})$	8192	8079	6080	4105
$\max(BW_{R^I;d})\%$	100%	98%	74%	50%
$\max(BW_{R^{II};d})$	7237	4183	3080	2084
$\max(BW_{R^{II};d})\%$	88%	51%	38%	25%
$\max(BW_{W^{II};d})$	2x6376	2x4183	2x3091	2x2097
$\max(BW_{W^{II};d})\%$	155%	101%	75%	51%

that is, the maximum memory accesses in the 1st and in the 2nd operational condition with writes is approximately the same for 70, 80 and 90 delays. Finally, we can note that:

$$\max(BW_{R^{II};70:90}) \approx \frac{\max(BW_{W^{II};70:90})}{2} \quad (3)$$

meaning that the memory read requests in the 2nd operational condition for 70,80 and 90 delays are halved due to L2WBs. This regulation choice is pessimistic because L2 writebacks does not always cause LLC writebacks and therefore writes to memory.

The results confirm an important hint for systematic MBA evaluation. When testing the memory bandwidth limitation for read operations, it is necessary to run measurements without L2 writebacks (first operational condition) capturing the most permissive limitation. In addition, we discovered that even though some delays do not contribute to the indirect memory bandwidth limitation in our setting, the delays 70, 80, and 90 have interesting behavior. Indeed, they limit and conserve their limitation even if there are memory writes. In particular, the 80 and 90 delays limit the synchronous memory bandwidth to 75% and 50%, respectively. In contrast, the 70 delay only avoids the overload of asynchronous requests due to L2WBs,

halving the synchronous bandwidth in the second operational condition.

These are important aspects to be considered when dimensioning a system with MBA in order to assure a given memory bandwidth to a critical core.

Along this direction, in the multicore analysis, we choose to evaluate the assured bandwidth when the MBA limits the interference workloads R^I only with 80 and 90 delays, covering the significant cases of synchronous bandwidth limitation.

VI. RESULTS FROM THE MULTI-CORE ANALYSIS

While the single-core analysis focused on the memory bandwidth limitation, we analyze the guaranteed bandwidth of a critical core when the MBA throttles the other cores in the multi-core analysis.

We analyze the delays that significantly limit the synchronous memory bandwidth: 80 and 90 delays reduce synchronous bandwidth by 75 and 50 percent, respectively. In addition, we design an interpretative model to explain the observed data.

We choose R^I as interfering workload, as motivated by the single-core analysis results. In the experiments, we deploy a quad-core system where all four cores start with empty private caches. In this way, the interference cores reproduce the R^I workload, while the critical core emulates a critical task that fills its private caches. In particular, the critical task fetches 512KB, while the interference cores 768KB, to be sure to last longer than the critical task.

In Table V, we associate an interference degree id to each experiment combination considering the limitation calculated in the single-core analysis.² An interference degree, for us, represents the synchronous memory accesses that we would execute without interference. If that load equals the number of requests performed by a single-core with a maximum rate, then the interference degree is equivalent to one.

The interference degree considers only the limitation of the single-core analysis and not the observed interference. Hence, for instance, the third combination of Table V, where two cores interfere with 80-delays (75% of synch. bandwidth) and one core with 90-delay (50% of synch. bandwidth), has the same interference degree of two cores that interfere without limitation. In Fig. 5, we report the boxplots of our critical latency observations for each combination of interference degrees in Table V, and we interpolate the 95-percentile. As expected, the lower the interference degree (achieved with high MBA delays) the lower the impact on the latency of the critical workload.

To better interpret this result, we also report the interpolation of the 95-percentile of the critical core latency when having exactly 1, 2 or 3 interfering cores with 0-delay, that is, no MBA limitation (blue line of Fig. 5).

Comparing the two 95-percentile interpolations, we can see how the MBA is effective at limiting the interference. For instance, when the interference degree is set to 2 (with 1

²Note that we are assuming the combinations position-independent (i.e., if we limit core 1 memory accesses, we suppose to be the same of limiting the core 2).

TABLE V
CRITICAL CORE LATENCY VARIABILITY WHEN THE THREE INTERFERENCE CORES ARE THROTTLED BY 80 OR 90 DELAY

#80d	#90d	interference degree id calculation	resulting id
0	3	$(0 * (3/4) + 3 * (1/2))$	1.5
1	2	$(1 * (3/4) + 2 * (1/2))$	1.75
2	1	$(2 * (3/4) + 1 * (1/2))$	2
3	0	$(3 * (3/4) + 0 * (1/2))$	2.25

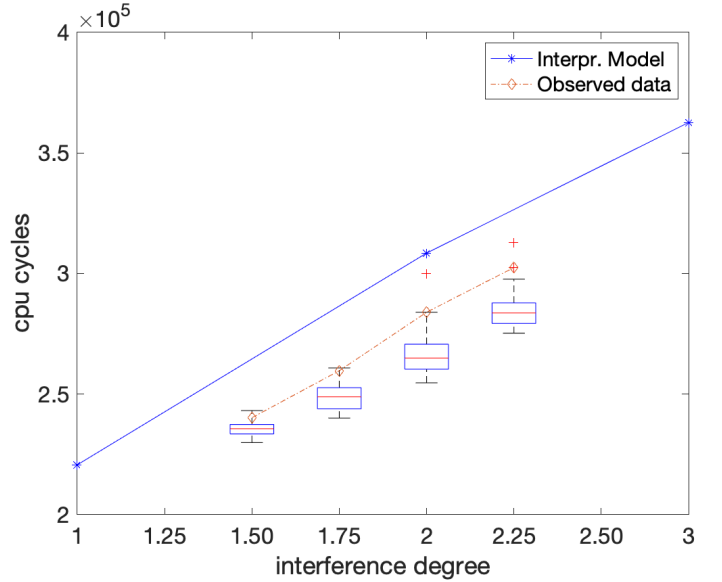


Fig. 5. Comparison between the critical execution latencies of the interpretative model and those observed as the degree of interference varies

interfering core with 90-delay and 2 interfering cores with 80-delay) the MBA is able to reduce the interference of 3 cores to at most the one we would have with 2 interference cores running without limitation. The blue line can thus be seen as the worst-case memory access latency we can achieve, when varying the interference degree, which is useful to establish a predictable behavior of the critical workload when run in a cloud system. This worst-case line is also easily achievable, from a practical point of view, by running interfering workloads with an increasing number of cores with no MBA.

Hence, our experiments show that the MBA can provide several safety upper bounds for the memory fetching phase of a critical task in a mixed-criticality Cloud infrastructure. Such bounds can be used in the WCET analysis of real-time tasks, without requiring invasive interventions to task code or execution. In particular, this solution doesn't require to modify the program of non-critical task to respect execution models (contrarily to [19], [3]) and it preserves private resource utilization limiting only the access versus the shared context (contrarily to software solutions such as Memguard [25] which halt the core execution).

VII. CONCLUSIONS AND FUTURE WORK

MBA is an interesting and reliable hardware feature for resource limitation in real-time systems. It can be used to regulate the access contention by limiting the arrival rate of the single physical cores. In this paper, we provide a systematic approach to estimate the indirect limitation of the MBA using three main workloads: memory reads with no L2 writebacks, memory reads with L2 writebacks and memory reads with L2 writebacks and memory writes. With experiments conducted on real hardware we discover that a good approach to measure the limitation in the worst-case is to run measurements without L2 writebacks. In addition, we found that only the Intel's 70, 80, and 90 delays values lead to significant limitations in our setting. Such limitation for the maximum synchronous bandwidth continues to be valid when there are memory writes, differently from state-of-the-art software-based solutions such as Memguard [25]. Our evaluation in the multi-core analysis showed that the MBA is able to provide memory bandwidth isolation for a critical task under heavy memory-intensive workloads on multi-core platforms. In addition, the MBA enables short regulation periods that would be hardly achievable with software-based methods. Finally, the MBA hardware limitation does not require to stop the execution of interfering cores to prevent memory accesses, and it does not require to execute the periodic regulation subroutine, improving the overall efficiency. Although results are achieved for a specific processor, we believe the proposed method is general enough to be applicable on different processor models. In the future, we plan to design a MBA-based approach to regulate the memory demand based on the current status of the memory controller and requirements of critical tasks, by dynamically assigning the required delay to interference cores, approaching an efficient regulation algorithm.

ACKNOWLEDGEMENTS

This work has been supported by the project COSMIC of UNINA DIETI.

REFERENCES

- [1] Frank Bellosa. Process cruise control: Throttling memory access in a soft real-time environment. In *SOSP 1997*, 1997.
- [2] Frank Bellosa. The third dimension of scheduling. 1999.
- [3] F. Boniol, H. Cassé, É. Noulard, and C. Pagetti. Deterministic execution model on cots hardware. In *ARCS*, 2012.
- [4] Sudipta Chattopadhyay, Lee Kee Chong, Abhik Roychoudhury, Timon Kelter, P. Marwedel, and H. Falk. A unified wcet analysis framework for multi-core platforms. In *IEEE Real-Time and Embedded Technology and Applications Symposium*, 2012.
- [5] Sudipta Chattopadhyay and Abhik Roychoudhury. Scalable and precise refinement of cache timing analysis via path-sensitive verification. *Real-Time Systems*, 49:517–562, 2013.
- [6] Sudipta Chattopadhyay, Abhik Roychoudhury, and T. Mitra. Modeling shared cache and bus in multi-cores for timing analysis. In *SCOPES*, 2010.
- [7] Marcello Cinque, Domenico Cotroneo, Luigi De Simone, and Stefano Rosiello. Virtualizing mixed-criticality systems: A survey on industrial trends and issues. *Future Generation Computer Systems*, 129:315–330, 2022.
- [8] Ericsson. *Network Compute Fabric*. Last accessed:08/21.
- [9] Gautam Gala, Gerhard Fohler, Peter Tummelshammer, Stefan Resch, and Reingard Hametner. RT-cloud: Virtualization technologies and cloud computing for railway use-case. In *24th IEEE International Symposium On Real-Time distributed Computing (IEEE ISORC)*. IEEE, 2021.
- [10] Intel. *IntelResource Director Technology (Intel RDT) On 2nd Generation Intel Xeon Scalable Processor Reference Manual*. April 2019.
- [11] Intel. *Intel 64 and IA-32 Architectures Software Developer's Manual*. November 2020.
- [12] Timon Kelter, H. Falk, P. Marwedel, Sudipta Chattopadhyay, and Abhik Roychoudhury. Bus-aware multicore wcet analysis through tdma offset bounds. *2011 23rd Euromicro Conference on Real-Time Systems*, pages 3–12, 2011.
- [13] O. Kotaba, Jan Nowotsch, M. Paulitsch, Stefan M. Petters, and Henrik Theiling. Multicore in real-time systems temporal isolation challenges due to shared resources. In *DATE 2013*, 2013.
- [14] Yun Liang, Huping Ding, T. Mitra, Abhik Roychoudhury, Y. Li, and V. Suhendra. Timing analysis of concurrent programs running on shared cache multi-cores. *Real-Time Systems*, 48:638–680, 2009.
- [15] Thomas Lundqvist and P. Stenström. Timing anomalies in dynamically scheduled microprocessors. *Proceedings 20th IEEE Real-Time Systems Symposium (Cat. No.99CB37054)*, pages 12–21, 1999.
- [16] Paolo Modica, Alessandro Biondi, Giorgio Buttazzo, and Anup Patel. Supporting temporal and spatial isolation in a hypervisor for ARM multicore platforms. In *Proc. ICIT*, pages 1651–1657. IEEE, 2018.
- [17] Paolo Walter Modica, Alessandro Biondi, Giorgio C. Buttazzo, and Anup Patel. Supporting temporal and spatial isolation in a hypervisor for arm multicore platforms. *2018 IEEE International Conference on Industrial Technology (ICIT)*, pages 1651–1657, 2018.
- [18] Jan Nowotsch and Michael Paulitsch. Quality of service capabilities for hard real-time applications on multi-core processors. In *Proceedings of the 21st International Conference on Real-Time Networks and Systems, RTNS '13*, page 151–160, New York, NY, USA, 2013. Association for Computing Machinery.
- [19] R. Pellizzoni, E. Betti, Stanley Bak, Gang Yao, J. Criswell, M. Caccamo, and R. Kegley. A predictable execution model for cots-based embedded systems. *2011 17th IEEE Real-Time and Embedded Technology and Applications Symposium*, pages 269–279, 2011.
- [20] R. Pellizzoni, A. Schranzhofer, Jian-Jia Chen, M. Caccamo, and L. Thiele. Worst case delay analysis for memory interference in multi-core systems. *2010 Design, Automation & Test in Europe Conference & Exhibition (DATE 2010)*, pages 741–746, 2010.
- [21] Jan Reineke, B. Wachter, Stephan Thesing, R. Wilhelm, I. Polian, J. Eisinger, and B. Becker. A definition and classification of timing anomalies. In *WCET*, 2006.
- [22] Siemens AG. Jailhouse hypervisor source code.
- [23] Sisu Xi, Meng Xu, Chenyang Lu, Linh TX Phan, Christopher Gill, Oleg Sokolsky, and Insup Lee. Real-time multi-core virtual machine scheduling in xen. In *Proc. EMSOFT*, pages 1–10. IEEE, 2014.
- [24] H. Yun, Gang Yao, R. Pellizzoni, M. Caccamo, and L. Sha. Memory access control in multiprocessor for real-time systems with mixed criticality. *2012 24th Euromicro Conference on Real-Time Systems*, pages 299–308, 2012.
- [25] H. Yun, Gang Yao, R. Pellizzoni, M. Caccamo, and L. Sha. Memguard: Memory bandwidth reservation system for efficient performance isolation in multi-core platforms. *2013 IEEE 19th Real-Time and Embedded Technology and Applications Symposium (RTAS)*, pages 55–64, 2013.